Supplement of Atmos. Chem. Phys. Discuss., 15, 24179–24215, 2015
http://www.atmos-chem-phys-discuss.net/15/24179/2015/
doi:10.5194/acpd-15-24179-2015-supplement

Atmospheric Chemistry and Physics Discussions

Supplement of

NO_x lifetimes and emissions of hotspots in polluted background estimated by satellite observations

F. Liu et al.

Correspondence to: S. Beirle (steffen.beirle@mpic.de) and Q. Zhang (qiangzhang@tsinghua.edu.cn)

1. Impact of interfering sources on a simple lifetime fit

In recent studies, the decay of NO_2 downwind from strong NO_x emission sources was used to derive the NO_x lifetime. However, this method can be strongly affected by neighboring sources. In a case study, we investigated the effect of an interfering source 100 km downwind with 10% of the emission rate as the source of interest. If such an interference is not accounted for by the fitted model function (e.g. in Beirle et al., 2011), the fit tries to "explain" the downwind interference by a higher lifetime. In the example shown in Fig. S1, a 10% of interference results in a 20% longer lifetime.

2. Investigated Locations

In this study, 24 power plants and 69 cities across China and the US are investigated, including 7 power plants and 16 cities located in mountainous regions, as listed in Table S2.

Table S2 Summary of power plants and cities investigated in this study.

Category	ID	Location	Latitude	Longitude	Lifetime	Emission (mol/s)	
						This Study	Bottom-up
Power Plants	1	Shangdu	42.2	116.0	2.3	20	17
	2	Shimen	29.6	111.4	3.6	7	8
	3	Tuoketuo	40.2	111.4	3.7	56	57
	4	Xinyang	32.1	114.1	3.3	8	11
	5	Xuzhou	34.4	117.3	5.4	63	58
	6	Yangcheng	35.5	112.6	7.5	30	24
	7	Colstrip	45.9	-106.6	3.7	11	14
	8	Conemaugh	40.5	-79.1	3.7	13	19
	9	Coronado	34.5	-109.3	2.0	9	9
	10	Crystal River	29.0	-82.7	3.1	13	16
	11	George Neal North	42.3	-96.4	2.5	15	11
	12	Harllee Branch	33.2	-83.3	4.4	12	12
	13	Hunter	39.3	-111.1	2.1	29	19
	14	Joppa Steam	37.2	-88.9	3.4	12	15
	15	Laramie River	42.1	-104.9	1.9	16	11
	16	Powerton	40.6	-89.6	3.9	11	13
	17	Rockport	37.9	-87.0	3.3	19	16
Cities	18	Pingdingshan	33.7	113.2	4.2	69	46
	19	Changchun	43.9	125.4	3.8	37	94
	20	Changsha	27.9	113.0	3.5	39	51
	21	Changzhi	36.3	113.2	3.4	65	42
	22	Chongqing	29.5	106.3	3.2	88	44
	23	Dalian	39.0	121.8	5.1	41	60

24	Daqing	46.6	125.1	3.8	26	88
25	Hangzhou	30.2	120.4	4.3	60	69
26	Harbin	45.8	126.7	3.5	58	72
27	Huainan	32.7	117.0	5.2	41	52
28	Jinan	36.9	117.9	6.4	181	79
29	Jiujiang	29.8	116.0	2.7	33	27
30	Kunming	25.0	102.8	3.9	23	50
31	Linyi	35.1	118.3	5.3	16	40
32	Liuzhou	24.3	109.4	2.8	26	31
33	Nanning	22.8	108.4	3.7	10	20
34	PRD	22.8	113.5	3.7	433	493
35	Qingdao	36.1	120.2	4.2	70	76
36	Qiqihar	47.2	123.6	4.3	20	27
37	Shanghai	31.3	121.5	4.7	322	271
38	Tangshan	39.7	118.2	3.9	162	141
39	Tianjin	39.1	117.3	3.7	145	100
40	Tonghua	41.8	126.0	3.6	16	15
41	Wuhan	30.6	114.3	2.6	185	130
42	Xiamen	24.5	118.1	3.4	89	72
43	Xiangyang	32.0	112.1	2.9	41	39
44	Yinchuan	38.5	106.2	3.5	33	28
45	Yueyang	29.4	113.1	2.6	28	24
46	Zhanjiang	21.3	110.3	3.7	11	22
47	Atlanta	33.8	-84.4	5.1	29	35
48	Chicago	41.8	-87.7	3.9	209	92
49	Cincinnati	39.1	-84.6	4.2	43	22
50	Cleveland	41.5	-81.7	4.6	11	33
51	Columbus	40.0	-83.1	5.6	7	22
52	Dallas	32.9	-97.0	3.9	77	39
53	Detroit	42.4	-83.1	4.5	100	61
54	Houston	29.8	-95.3	3.5	78	50
55	Indianapolis	39.8	-86.2	4.7	17	21
56	Jacksonville	30.5	-81.6	3.2	23	30
57	Kansas City	39.2	-94.6	3.5	32	27
58	Memphis	35.1	-90.1	3.0	11	21
59	Miami	26.0	-80.2	4.7	39	36
60	Minneapolis	45.0	-93.3	3.8	62	44
61	Montreal	45.6	-73.7	2.5	59	59
62	New Orleans	30.1	-90.3	4.9	15	14
63	New York	40.7	-73.5	4.4	247	311
64	Omaha	41.3	-96.1	2.0	32	25
65	Orlando	28.5	-81.3	3.5	24	25
66	Philadelphia	40.0	-75.2	4.4	55	65
67	San Antonio	29.6	-98.5	3.4	20	16

	68	St Louis	38.7	-90.4	3.7	56	36
	69	Tampa	27.9	-82.4	3.7	39	28
	70	Tucson	32.3	-110.9	1.8	21	11
Mountainous Power Plants	71	Daba	38.0	105.9	3.5	86	24
	72	Jingyuan	36.7	104.8	1.6	14	19
	73	Shentou	39.4	112.6	2.9	73	52
	74	Cholla	34.9	-110.3	1.9	21	8
	75	Four Corners	36.8	-108.4	2.2	83	44
	76	Intermountain	39.5	-112.6	2.1	39	19
	77	Navajo	36.9	-111.4	3.1	18	22
Mountainous Cities	78	Baotou	40.6	109.8	4.3	94	82
	79	Beijing	39.8	116.3	2.5	252	109
	80	Chifeng	42.3	119.3	2.5	26	25
	81	Datong	40.1	113.3	3.3	106	70
	82	Hohhot	40.8	111.7	4.1	26	38
	83	Lanzhou	36.1	103.8	2.0	35	47
	84	Shijiazhuang	38.1	114.5	4.0	261	72
	85	Taiyuan	37.6	112.4	2.9	180	78
	86	Wenzhou	28.0	120.7	7.9	18	46
	87	Zhangjiakou	40.8	114.8	2.4	64	43
	88	Denver	39.8	-105.0	2.6	78	47
	89	Las Vegas	36.2	-115.2	1.7	68	31
	90	Phoenix	33.6	-112.0	1.3	138	36
	91	Portland	45.5	-122.6	2.8	73	33
	92	Salt Lake City	40.7	-112.0	1.9	87	20
	93	Seattle	47.4	-122.3	1.4	232	29

3. Uncertainties

We here investigate the different sources of uncertainties contributing to the overall uncertainties of the derived lifetimes and emissions. For both τ and emissions, the calculation of line densities (a), wind fields (b), potential dependence of lifetimes on wind conditions (c) and fit errors (d) contribute to the uncertainties. In addition, uncertainties in the total NO_2 mass fit (e), tropospheric NO_2 TVCDs and the NO_2/NO_x ratio (f) affect the derived emissions.

(a) Calculation of line densities

Analogue to Beirle et al. (2011), we investigate the impact of the a-priori choice of integration and fit intervals. The fitted τ is generally robust with respect to changes of the fit interval *f* and integration interval *i* for the calculation of *C(x)* in *N(x)*, associated with the good representation of the emission pattern provided by the NO_2 distribution under calm wind

condition $C(x)$ in any case. A change of f and i by ± 100 km affects the resulting lifetimes by only about 10%. The dependency of the fit results for τ and emissions on the fit and integration intervals and choice of wind fields are tabulated in Table S1.

(b) Wind fields

The accuracy of wind fields directly affects the results by providing direction information for sorting NO_2 TVCDs and relating the observed e-folding distance x_0 to the lifetime via $\tau = x_0/w$. We choose ECMWF wind fields averaged from ground up to 500 m and a threshold of 2 m/s for calm winds in this study. Uncertainties due to the choice of layer height (e.g. 200m or 1000 m) are comparable with Beirle et al. (2011): the resulting lifetimes/emissions change about 10% on average. We also investigate the dependency on the choice of the threshold for calm wind. The threshold of 2 m/s was found to be a good compromise of sufficient sample size for both the calculation of line densities for calm as well as for windy conditions. It successfully worked out for 70 non-mountainous sites, while for both lower and higher thresholds (of e.g. 1 m/s and 3 m/s), several sites are discarded, due to low sample sizes for calm (implying a bad representation of the emission pattern) and noisy downwind patterns, respectively. Thus we consider that the threshold of 2 m/s is optimal in this study.

In addition, we carried out a comparison of wind information between ECMWF and sounding measurements (Table S3). Here we focus on the comparison of the quantity used for the lifetime estimate, i.e. the projected wind components for each wind direction sector. We firstly sorted ECMWF wind fields for the years 2005–2013 into 8 wind direction sectors and classified the simultaneous sonde data into the same wind direction sector, and then calculate the mean of the projected wind speeds from both datasets to compare. Note that it is to be expected that the ECMWF wind components are systematically higher than those from independent datasets, as ECMWF wind fields are the basis for the wind direction classification. That is, deviations of the wind direction (even if 0 on average) cause a systematic bias due to this projection procedure. However, we do not try to correct for this potentially systematic effect, as the wind sonde data availability is limited (for some sites and only punctual, not covering the complete plume). The deviations for non-mountainous sites are acceptable (26%), but higher (37%) for mountainous sites due to insufficient spatial resolution of ECMWF.

Overall, we estimate the uncertainties associated with the wind data as 20% for non-mountainous sites, as it is expected to be less than the observed deviations between ECMWF and sond wind components (26%) due to the systematical bias discussed above.

(c) Potential dependence of lifetimes (and other factors) on wind conditions

We also checked the mean NO_2 TVCDs for calm and windy conditions (Fig. S5). We in fact observe systematic differences in NO_2 TVCDs between calm and windy conditions, which are likely related to changes in lifetimes under different wind conditions. Valin et al. (2013) argue that higher wind speeds cause faster dilution of NO_x, leading to longer lifetimes. This effect could contribute to the observed larger NO_2 TVCDs under windy conditions compared to calm wind conditions. However, it is interesting to note that the magnitudes of NO_2 TVCDs are larger under calm wind conditions for some sites. A better understanding of the dependence of NO_2 column densities on wind conditions requires more complex models, accounting for various parameters influencing the NO_x chemistry instead of merely wind speeds. The effect is rather small (less than 10% on average see Fig. S5), we thus estimate the uncertainties due to the potential dependence of lifetimes (and other factors) on wind conditions as 10%.

(d) Fit errors

The fit errors expressed as 95% confidence interval (CI) are derived from the fit results directly for individual sources. They are typically of the order of 30% for τ and 20% for A, respectively. In addition, for τ, the standard deviation of all wind direction sectors is regarded as a measure of uncertainty to reflect the reliability of lifetimes. But for 5 sites, the fit of τ can only work for a single direction, which misses the information of standard deviations. We average the standard deviations for all available sites and calculate the respective uncertainty as 40%, and apply the number to all considered sites.

(e) Fit of the total NO_2 mass

The integration interval aligned in the wind direction h and fit interval aligned in the across-wind direction v (see Fig. S2) was chosen in order to allow a robust fit of the total NO_2 mass on top of the background. If h and v are chosen too small, emissions are underestimated caused by the loss of part of the NO_2 TVCDs from the source of interest; while, if h and v are chosen too large, interferences from surroundings are included and the derived emissions are not from the target source, but from a larger area. The fitted emissions are rather insensitive to

the change of *v*, because possible losses by cross-wind dilution are accounted for by scaling the integrated NO_2 mass according to the fitted width of the Gaussian plume. The resulting emissions change about 5% on average when *v* is increased by 50%. If the fit interval *h* is increased by 50% as well, the emissions for fewer sites (66 sites) can be estimated, related to the enhanced interferences corresponding to larger *h* which cannot be simply interpreted by linear background (i.e., $\varepsilon_i+\beta_i x$ in Eq. (5)), thus justifying the choice of *h* as reasonable. The fitted emissions are also found to be not very sensitive to the choice of *h: A* increases by only ~20% when *h* increases by 150%. We estimate the uncertainties due to the fit of the total NO_2 mass as 20%, and apply this number to all considered sources.

(f) Tropospheric NO_2 TVCDs and the NO_2/NO_x ratio

The uncertainties of NO_2 TVCDs and NO_x/NO_2 are assumed to be 30% and 10% for emissions following the estimations in Beirle et al. (2011). Note that the lifetime estimation is not affected by these uncertainties.

Table S1. The mean relative change of resulting lifetime τ and emission E for different choices of fit and integration intervals, and wind fields.

	f+100	f−100	i+100	i−100	h×150%	v×150%	⩽1 m/s[a]	⩽3 m/s[a]	200m[b]	1000m[b]
mean[($\Delta\tau$)/τ]	-2%	-4%	7%	8%	—	—	-5%	2%	7%	-8%
mean[($\Delta\tau$)]/mean[τ]	-4%	-4%	6%	5%	—	—	-9%	2%	7%	-9%
mean[($\Delta\tau$)]	-0.2	-0.2	0.2	0.2	—	—	-0.3	0.1	0.3	-0.4
mean[(ΔE)/E]	7%	8%	-2%	2%	14%	1%	7%	0%	-5%	13%
mean[(ΔE)]/mean[E]	5%	5%	-3%	12%	22%	6%	0%	-1%	-3%	11%
mean[(ΔE)]	3.4	3.3	-2.2	7.3	13.2	0.6	-0.2	-0.5	-2.0	6.0
N[c]	69	70	69	69	66	69	19	64	67	69

[a]definition of calm wind

[b]the height that ECMWF wind fields averaged from ground up to

[c]the number of sources for which the modified method in this study can work out

1 Table S3. Comparison of average wind speeds for years 2005−2013 for available cities from
2 ECMWF and sounding measurements assembled by University of Wyoming.

City	Average Speed (m/s)[a]		Percentage Change[b]	r^2	Elevation Difference (m)[c]
	ECMWF	Sounding			
Miami	4.8	4.0	15%	0.59	0
Harbin	7.0	5.6	20%	0.67	-6
Wuhan	4.6	3.2	31%	0.63	25
Omaha	7.8	6.4	18%	0.77	33
Kunming	7.0	5.0	28%	0.72	36
Changsha	4.9	2.8	43%	0.61	73
Xiamen	6.2	5.0	19%	0.65	77
Chongqing	3.9	2.2	43%	0.30	85
Non-mountainous cities	5.8	4.3	26%	0.62	40
Chifeng	5.8	3.3	43%	0.42	273
Phoenix	3.6	3.0	18%	0.19	315
Beijing	4.5	3.9	14%	0.56	319
Lanzhou	4.7	2.4	48%	0.41	416
Salt Lake City	4.0	2.8	29%	0.30	479
Taiyuan	4.9	2.5	49%	0.42	410
Denver	3.5	1.8	50%	0.12	637
Mountainous cities	4.4	2.8	37%	0.35	429

[a]Average of wind speeds (>2 m/s) for each wind direction sector

[b]Percentage change = (speed in ECWMF−speed in sounding) / speed in ECWMF

[c]Elevation difference = elevation in ECWMF−elevation in GTOPO

Table S4. Topographic information of power plants and cities defined as mountainous sites.

ID	Location	Lifetime	Elevation in GTOPO (m)	Elevation in ECMWF (m)	Elevation Difference (m)
71	Daba	3.5	1121	1373	252
72	Jingyuan	1.6	1491	1824	333
73	Shentou	2.9	1057	1405	348
74	Cholla	1.9	1548	1838	290
75	Four Corners	2.2	1628	1918	290
76	Intermountain	2.1	1420	1671	250
77	Navajo	3.1	1358	1720	362
78	Baotou	4.3	1043	1331	288
79	Beijing	2.5	40	359	319
80	Chifeng	2.5	481	754	273
81	Datong	3.3	1027	1350	323
82	Hohhot	4.1	1046	1412	366
83	Lanzhou	2.0	1743	2159	416
84	Shijiazhuang	4.0	76	341	265
85	Taiyuan	2.9	799	1208	410
86	Wenzhou	7.9	18	329	311
87	Zhangjiakou	2.4	738	1203	465
88	Denver	2.6	1610	2247	637
89	Las Vegas	1.7	638	1031	393
90	Phoenix	1.3	339	654	315
91	Portland	2.8	67	364	297
92	Salt Lake City	1.9	1297	1776	479
93	Seattle	1.4	36	369	333

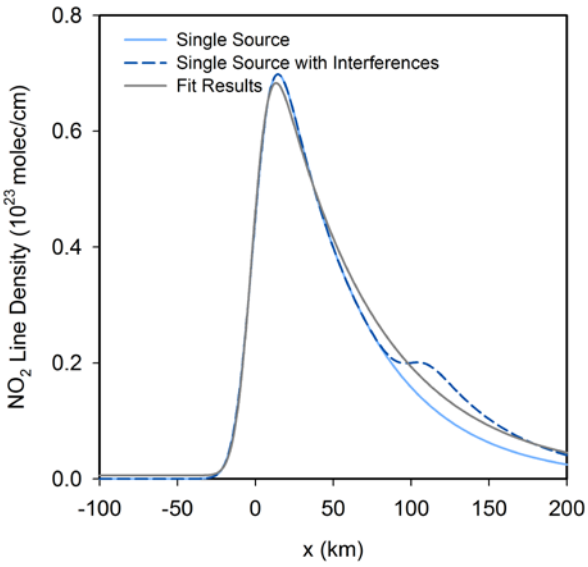

Figure S1. Sensitivity of the fitted lifetime to interferences. Solid blue line: synthetic line densities of a single source with emissions of 500 molec-NO_2/s, assuming a pseudo first-order loss of NO_2 for a a-priori lifetime of 3 hours and a wind speed of 5 m/s with a spatial smoothing following a Gaussian function with a standard deviation of 10 km; blue dash: line densities of the single source with an additional source with emissions of 50 molec-NO_2/s at 100 km. Grey: lifetime fit based on *M(x)* (Eq. 1).

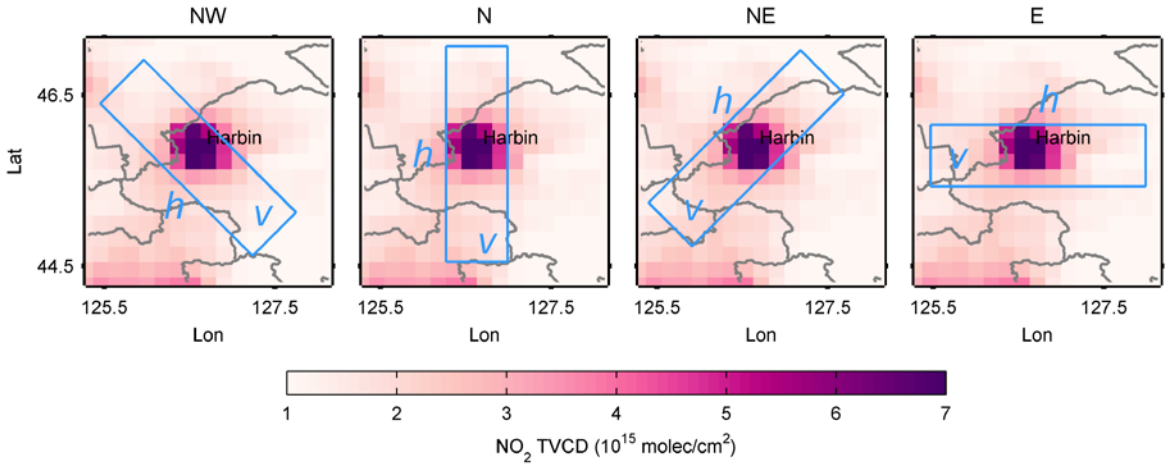

Figure S2. The intervals chosen for the fit of total NO_2 mass for northwest, north, northeast and east directions (from left to right). The mean calm NO_2 TVCDs are integrated in across-wind direction *v* to calculate line densities and the fit is performed over the interval *h* (see Sect. 2.2.3).

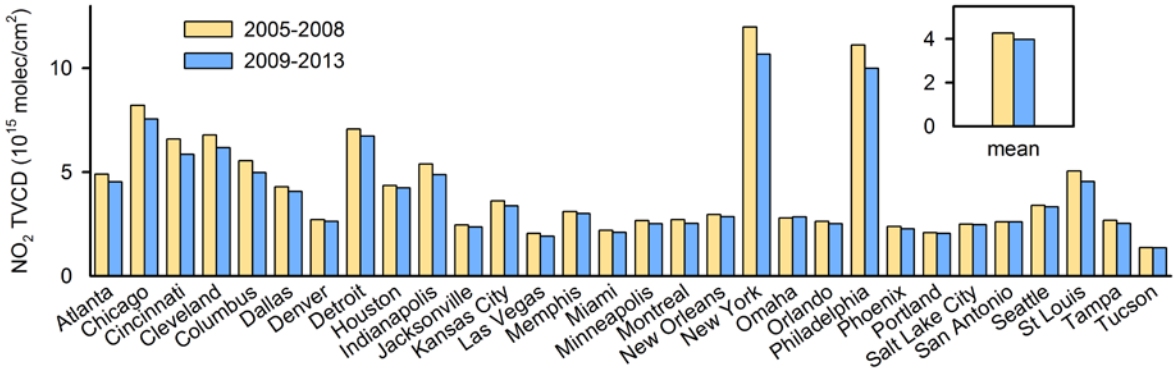

Figure S3. NO_2 TVCDs of investigated cities over the US. The yellow and blue bars denote the mean NO_2 TVCDs in a circle with a radius of 100 km around city centers for the ozone season during 2005–2008 and 2009–2013 respectively. The bars in the inset display the mean NO_2 TVCDs of cities shown.

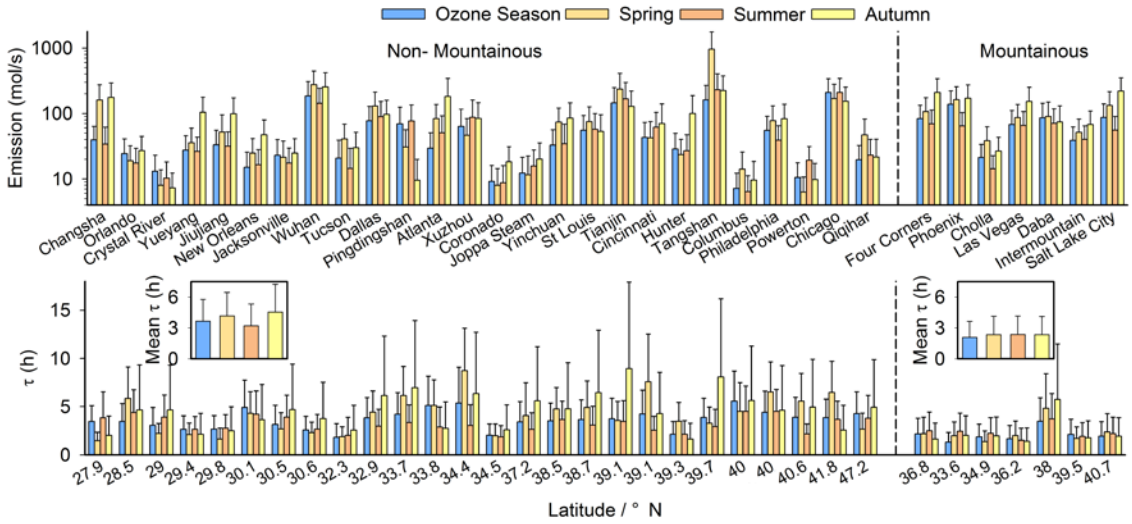

Figure S4. Seasonal mean NO_x emissions and lifetimes. Mean daytime NO_x emissions (top panel) and lifetimes (bottom panel) for the investigated sources (from south to north). The results for mountainous and non-mountainous sites are illustrated separately. The bars in the insets of the bottom panel display the average NO_x lifetimes of sources shown for each season. Error bars show the uncertainties.

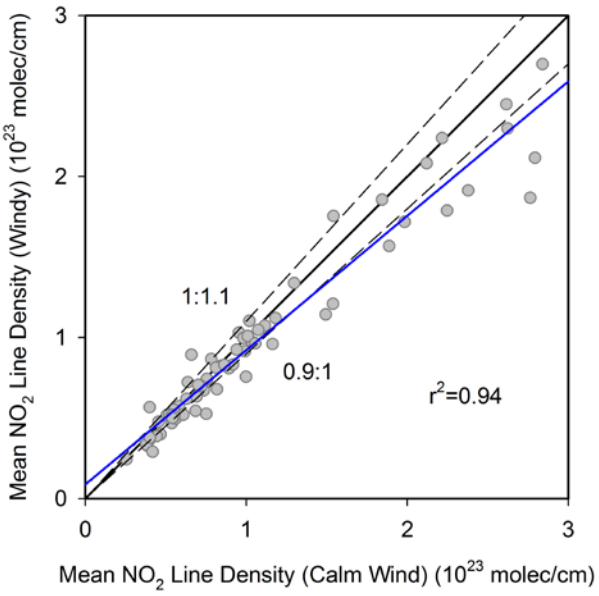

Figure S5. Scatterplot of mean NO_2 line densities under calm wind condition versus under windy condition. NO_2 line densities (integration interval: 300 km) for non-mountainous power plants and cities are averaged over the fit interval (600 km). Only those wind directions are included for which the fit works properly. The blue line represents the fitted regression line with a slope of 0.8 and an intercept of 0.1. The ratio of mean NO_2 line density under windy wind condition to that under calm wind condition is 0.9.

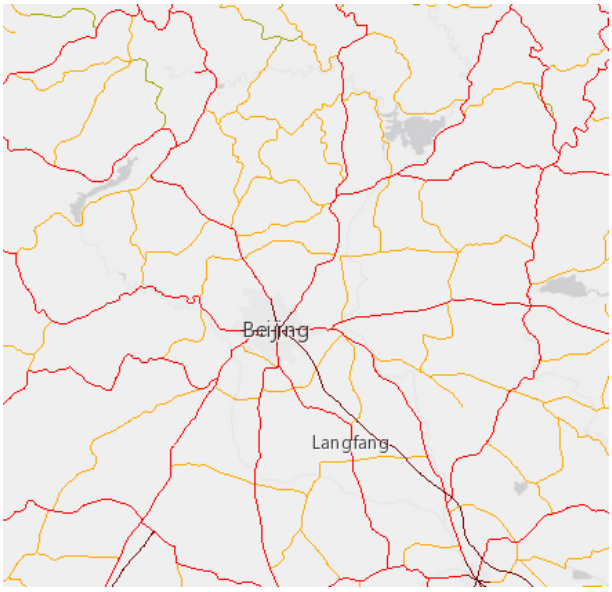

Figure S6. Road-network map of Beijing from the GRIP database. The map is a screen capture of the GRIP website (http://geoservice.pbl.nl/website/flexviewer/index.html?config=cfg/PBL_GRIP.xml).